# Opiate-mediated inhibition of calcium signaling is decreased in dorsal root ganglion neurons from the diabetic BB/W rat.

K E Hall, … , A A Sima, J W Wiley

*J Clin Invest.* 1996;97(5):1165-1172. https://doi.org/10.1172/JCI118530.

**Research Article**

The effect of diabetes mellitus on opiate-mediated inhibition of calcium current density (I(D Ca) [pA pF-1]) and cytosolic calcium response ([Ca2+]i nM) to depolarization with elevated KCl and capsaicin was assessed. Experiments were performed on isolated, acutely dissociated dorsal root ganglion (DRG) neurons from diabetic, BioBreeding/Worcester (BB/W) rats and age-matched control animals. Sciatic nerve conduction velocity was significantly decreased in diabetic animals compared to controls. Mean I(DCa) and [Ca2+]i responses to capsaicin and elevated KCl recorded in DRGs from diabetic animals were significantly larger than those recorded in DRG neurons from controls. In neurons from diabetic animals, the opiate agonist dynorphin A (Dyn A; 1, 3, and 5 microM) had significantly less inhibitory effect on I(D Ca) and KCl-induced [Ca2+]i responses compared to controls. Omega-conotoxin GVIA (omega-CgTX; 10 microM) and pertussis toxin (PTX; 250 ng ml-1) abolished Dyn A-mediated inhibition of I(DCa) and [Ca2+]i in control and diabetic neurons, suggesting that Dyn A modulated predominantly N-type calcium channels coupled to opiate receptors via PTX-sensitive (Gi/o) inhibitory G proteins. These results suggest that opiate-mediated regulation of PTX-sensitive, G protein-coupled calcium channels is diminished in diabetes and that this correlates with impaired regulation of cytosolic calcium.



# Opiate-mediated Inhibition of Calcium Signaling Is Decreased in Dorsal Root Ganglion Neurons from the Diabetic BB/W Rat

**Karen E. Hall,* Anders A.F. Sima,*‡§ and John W. Wiley*‖**

*Departments of *Internal Medicine and ‡Pathology, and §Michigan Diabetes Research and Training Center, University of Michigan; and ‖Ann Arbor Veterans Administration Hospital, Ann Arbor, Michigan 48109*

## Abstract

**The effect of diabetes mellitus on opiate-mediated inhibition of calcium current density ($I_{DCa}$ [pA $pF^{-1}$]) and cytosolic calcium response ($[Ca^{2+}]_i$ nM) to depolarization with elevated KCl and capsaicin was assessed. Experiments were performed on isolated, acutely dissociated dorsal root ganglion (DRG) neurons from diabetic, BioBreeding/Worcester (BB/W) rats and age-matched control animals. Sciatic nerve conduction velocity was significantly decreased in diabetic animals compared to controls. Mean $I_{DCa}$ and $[Ca^{2+}]_i$ responses to capsaicin and elevated KCl recorded in DRGs from diabetic animals were significantly larger than those recorded in DRG neurons from controls. In neurons from diabetic animals, the opiate agonist dynorphin A (Dyn A; 1, 3, and 5 μM) had significantly less inhibitory effect on $I_{DCa}$ and KCl-induced $[Ca^{2+}]_i$ responses compared to controls. Omega-conotoxin GVIA (ω-CgTX; 10 μM) and pertussis toxin (PTX; 250 ng $ml^{-1}$) abolished Dyn A–mediated inhibition of $I_{DCa}$ and $[Ca^{2+}]_i$ in control and diabetic neurons, suggesting that Dyn A modulated predominantly N-type calcium channels coupled to opiate receptors via PTX-sensitive ($G_{i/o}$) inhibitory G proteins. These results suggest that opiate-mediated regulation of PTX-sensitive, G protein–coupled calcium channels is diminished in diabetes and that this correlates with impaired regulation of cytosolic calcium. (*J. Clin. Invest.* 1996. 97:1165–1172.) Key words: diabetic neuropathy • opiate • calcium current • cytosolic calcium • G protein**

## Introduction

Diabetic neuropathy is the most common form of peripheral neuropathy in the Western world, with metabolic, functional, and morphological changes in peripheral nerves documented in both human and animal models of diabetes mellitus (1–5). Many of the abnormalities described in peripheral nerves of animal and human diabetics, such as decreased conduction velocity, axonal swelling, axo-glial dysjunction, and nerve fiber loss (1, 6) have been linked to metabolic alterations such as decreased myo-inositol tissue levels, decreased $Na^+$,$K^+$-ATPase activity, mitochondrial dysfunction, and altered calcium signaling (7–9).

Considerable evidence suggests that metabolic over-stimulation by cytosolic calcium ($[Ca^{2+}]_i$)[1] may contribute to neuronal cell injury (10). Diabetes has been correlated with impaired calcium signaling in many tissues from diabetic animals (8). An important contribution to $[Ca^{2+}]_i$ in neurons is made by the entry of external $Ca^{2+}$ through voltage-dependent calcium channels (11). We recently reported enhancement of multiple, voltage-dependent whole-cell calcium currents ($I_{Ca}$) in acutely dissociated, capsaicin-sensitive dorsal root ganglion (DRG) neurons from the spontaneously diabetic BioBreeding/Worcester (BB/W)-rat model of type I human diabetes mellitus (9). The magnitude of the current enhancement increased with the duration of diabetes and nerve conduction velocity slowed. Both abnormalities were prevented by long-term oral treatment of diabetic animals with an aldose reductase inhibitor.

Endogenous opiates, such as dynorphin A (Dyn A), have been detected in dorsal root ganglia from adult rats (12), and local release of opiate transmitters may play an important role in modulating neurotransmission in primary afferent pathways. Decreased sensitivity to opiates at the spinal level, as evidenced by decreased inhibition of tail flick response to noxious stimuli (13) and impaired vagal transport of opiate receptors (14) have been previously demonstrated in diabetic animal models. However, the cellular mechanism(s) underlying the decreased neuronal response to opiates in diabetes are unknown. Because previous studies suggested that calcium channels were affected in diabetes mellitus (9), we hypothesized that altered opiate-mediated regulation of neuronal calcium channels might contribute to the changes in calcium signaling observed in diabetes. Activation of κ and μ opiate receptors on DRG neurons inhibits calcium influx through voltage-activated calcium channels via a pertussis-sensitive, inhibitory ($G_{i/o}$) G protein–coupled pathway (15–17). We compared the inhibitory effect of the opiate agonist Dyn A on whole-cell, voltage-dependent calcium current density ($I_{DCa}$) and $[Ca^{2+}]_i$ in acutely dissociated DRG neurons from diabetic and age-matched nondiabetic animals. $[Ca^{2+}]_i$ was monitored using the Fura-2 method, to determine whether the increase in $I_{DCa}$ observed in diabetes was associated with parallel alterations in $[Ca^{2+}]_i$. These studies have been presented in preliminary form (18).

## Methods

*Animal model.* Prior approval for these experiments was obtained from the University of Michigan Committee on Use and Care of Ani-

Address correspondence to Karen E. Hall, Medical Science Research Building I, Room 65200, 1150 Medical Center Drive, Ann Arbor, MI 48109-0682. Phone: 313-747-2941; FAX: 313-763-2535; E-mail: kehall@umich.edu

*Received for publication 10 July 1995 and accepted in revised form 6 December 1995.*

The Journal of Clinical Investigation
Volume 97, Number 5, March 1996, 1165–1172

1. *Abbreviations used in this paper:* $[Ca^{2+}]_i$, cytosolic calcium; DRG, dorsal root ganglion; Dyn A, dynorphin A; PTX, pertussis toxin.

mals (Authorization No. 3593A[2]), according to National Institutes of Health (NIH) guidelines. Two groups of male BB/W-rats were used: (*a*) adult, nondiabetic controls aged 9–13 mo and (*b*) age-matched diabetic rats treated with daily insulin injection (diabetic duration 7–10 mo). Prediabetic and non–diabetes-prone animals were obtained from the NIH-sponsored colony at the University of Massachusetts (Worcester, MA) and maintained at the Michigan Diabetes Research and Training Center. After the onset of diabetes (as determined by glucosuria during daily urine glucose monitoring), ultralente insulin (0.4–3.0 IU $d^{-1}$; Novo Nordisk, Princeton, NJ) was administered subcutaneously daily to maintain hyperglycemic blood glucose levels between 16 and 25 mM $liter^{-1}$ (300–450 mg $dl^{-1}$) and prevent ketoacidosis. Body weight, urinary glucose, and ketone bodies were monitored daily, and the insulin dose titrated as described previously (19). Blood glucose levels were monitored daily until the desired plasma glucose levels were achieved, and biweekly thereafter. Shortly after onset of diabetes, a subset of six diabetic animals had recording electrodes implanted on the left sciatic nerve for measurement of nerve conduction velocity (5). An equal number of nondiabetic, age-matched control animals were similarly prepared. Nerve conduction velocity was measured within 2 wk of killing.

*Cell dissociation.* Isolated, acutely dissociated DRG neurons were aseptically prepared from animals diabetic for 7–10 mo or age-matched control animals using techniques described previously (9). Thoracic DRGs were extracted from the spinal column, trimmed, minced, and incubated with 0.3% collagenase type II (Sigma Chemical Co., St. Louis, MO) and 0.1% bovine trypsin type I (Sigma) prepared in sterile MEM (GIBCO BRL, Grand Island, NY) supplemented with 16 mM $NaHCO_3$ and 28 mM D-glucose (320 mosmol $kg^{-1}$). After enzyme treatment, the minced DRGs were triturated and centrifuged to produce isolated neurons. After resuspension in supplemented MEM containing 10% horse serum (GIBCO), neurons were plated onto poly-L-lysine-coated glass coverslips. Nerve growth factor was not added to the culture medium. Coverslips were incubated in 93% air + 7% $CO_2$ at 37°C for 1.5–7 h before experiments were performed.

*Drug preparation.* Omega-conotoxin GVIA (ω-CgTx) 1 mM stock solution (Sigma Chemical Co.) was prepared with filtered distilled water, lyophilized in 10 μl aliquots, and stored at −20°C. On the recording day, 10 μM ω-CgTx was prepared by diluting the lyophilized stock with external recording solution. Capsaicin stock solution (10 mM; Sigma) in 95% ethanol was stored at 4°C. On the experimental day, concentrations of 0.1 and 1 μM capsaicin were prepared by diluting the stock solution with electrophysiologic external recording solution and Fura-2 recording medium, respectively. Dyn A (Peninsula Laboratories, Inc., Belmont, CA) was diluted to 10 mM with distilled water containing 0.1% acetic acid, lyophilized, and stored at −20°C. On the recording day, working solutions of Dyn A (1, 3, and 5 μM) were made by dilution either with external recording solution containing 0.1% BSA (Sigma) for application during electrophysiologic recording, or Fura-2 recording medium for application during measurement of $[Ca^{2+}]_i$. The above working solutions were kept on ice until used. In experiments testing the effects of pertussis toxin (PTX; Sigma), culture dishes were preincubated with medium containing 250 ng $ml^{-1}$ PTX for 3–4 h before recording.

*Whole-cell voltage-clamp recordings.* Phase-bright DRGs, 20–40 mm in diameter, were selected using a micrometer in the microscope objective. Voltage-clamp recordings using the whole-cell variant of the patch clamp technique (20) were performed at room temperature with glass recording patch pipettes (Fisher Microhematocrit tubes; Fisher Scientific Co., Pittsburgh, PA). Electrode resistances were 1–2 MΩ, and seal resistances > 1 GΩ. Experiments were performed in a nonperfused culture dish containing the following external bath solution: (mM) 5 $CaCl_2$, 67 choline Cl, 100 tetraethylammonium chloride, 5.6 glucose, 5.3 KCl, 10 Hepes, and 0.8 $MgCl_2$ (pH 7.3–7.4, 320–330 mosmol $kg^{-1}$). Recording electrodes were filled with (mM) 140 cesium Cl, 10 Hepes, 10 EGTA, 5 MgATP, and 0.1 LiGTP (all reagents from Sigma Chemical Co.). The pH was adjusted to 7.2–7.3 with 1 M CsOH after addition of ATP and GTP, and the final osmolality (280–290 mosmol $kg^{-1}$) was adjusted to 10–15% below that of the external recording solution using distilled water. High-threshold calcium currents were elicited by depolarizing voltage steps generated using the program CLAMPEX (pCLAMP; Axon Instruments, Foster City, CA). Currents were recorded using an Axopatch 1D patch clamp amplifier (Axon Instruments) with an input resistance of 1–3 MΩ, filtered with a Bessel filter at 10 kHz (−3 decibels), sampled at 20 kHz, and stored on hard disk as binary data files. Neurons were clamped at a holding potential ($V_h$) = −80 mV. Immediately after patch rupture, 10 depolarizing calibration voltage steps (+5 mV; 12 ms duration) were applied at 1 s intervals. High-threshold currents were evoked at 30 s intervals by 100 ms duration depolarizations to +10 mV. The total duration of recording was ∼ 20 min from the time of patch rupture. Currents elicited by the depolarization protocol described above increased in amplitude by 20–30% for the first 3–5 min ("runup"), then steadily decreased to ∼ 60% of their maximum amplitude by 20 min ("rundown"). Because each cell varied in the time at which the maximal current amplitude was recorded, Dyn A was applied when the currents had finished the runup phase and were just beginning to decrease, rather than at a set time after patch rupture. This was done to minimize variability in Dyn A–mediated inhibition of currents between diabetic and control animals that might be due simply to underlying current runup or rundown. After eliciting a current using the protocol described above (pre–Dyn A current), Dyn A prepared as described above was applied to the isolated cells using pressure ejection (compressed air; 0.5 psi) from a glass micropipette "puffer" with 10–40 μm tip opening positioned ∼ 50 mm from the neuron being recorded. The drug pipette was lowered into the bath immediately before a 2 s application of drug. Currents were evoked by the depolarization protocol described above at 2 and 15 s after drug application (post–Dyn A currents). If the inhibitory response to Dyn A at 15 s was larger than the response at 2 s (suggesting that the full effect of that drug concentration was delayed or might be submaximal), a second application of the same drug concentration for 3 s was performed 30 s after the first application. Currents were elicited 2 s after the second application, after which the drug pipette was removed from the bath. Currents were elicited at 30-s intervals until recovery from the drug effect was maximal, then ω-CgTx (10 mM) was applied using a second micropipette puffer with the same protocol as described for the Dyn A application. In neurons in which currents could still be elicited after administration of ω-CgTx, 0.1 μM capsaicin was applied via a third micropipette to assess capsaicin sensitivity, defined as a reduction of > 10% in current amplitude.

*Analysis of calcium currents.* Binary data files were analyzed with the program CLAMPAN. Leak currents assessed by hyperpolarizing commands of equal value to those used to depolarize the cell were digitally subtracted from $I_{Ca}$. There was no significant difference in the leak currents measured in control (68±44 pA; $n$ = 24) and diabetic neurons (87±32 pA; $n$ = 20). To control for the possibility that alterations in $I_{Ca}$ between the control and diabetic groups occurred simply on the basis of variations in cell size, the current density ($I_{DCa}$ [pA $pF^{-1}$]) was determined. 10 small depolarizing calibration voltage pulses ($V_c$ = +5 mV for 12 ms) performed immediately after patch rupture were averaged, and whole cell capacitance (proportional to surface area) was calculated using the following formula:

$$C = AV^{-1}$$

where $C$ = capacitance (pF), $A$ (pF $mV^{-1}$) = the area under the capacitance current curve from the peak inward current to the point at which $I_{Ca}$ = 0, and $V$ = calibration voltage step (mV). Peak inward currents were divided by the cell capacitance, and the normalized current density ($I_{DCa}$) expressed in units of pA $pF^{-1}$. The percent inhibition caused by Dyn A application was calculated using the following formula:

$$(1 - [\{\text{Post-Dyn A } I_{DCa}\} / \{\text{Pre-Dyn A } I_{DCa}\}]) \cdot 100$$

where Pre-Dyn A $I_{DCa}$ was the current recorded immediately before lowering the drug micropipette into the bath, and Post-Dyn A $I_{DCa}$ was the lower of the two currents elicited at 2 and 15 s after Dyn A application. The difference between the resulting fraction and 1 was calculated and expressed as a percentage of 100.

*Measurement of $[Ca^{2+}]_i$.* Using the Fura-2 technique (21), $[Ca^{2+}]_i$ was measured in DRGs prepared as described above. Coverslips were incubated for 2 h in MEM containing 1 μM Fura-2 AM (acetoxymethyl ester and free acid; Molecular Probes, Eugene, OR) at 37°C in a light-tight water bath, then placed into a perfusion chamber on the stage of an inverted microscope (Nikon Inc., Melville, NY) and superfused continuously with oxygenated Krebs buffer at 37°C. On each coverslip, a single isolated, phase-bright DRG in the size range of interest (20–40 μm) was selected using a micrometer in the ocular of the microscope. To avoid any bias due to decreased responsiveness to depolarization in neurons previously depolarized, only one neuron was studied on each coverslip. Fluorescence was elicited by illumination with light wavelengths alternating between 340 and 380 nm at 0.5 s intervals. Fluorescence was recorded using a SPEX fluorescence detection apparatus (SPEX DM 3000; SPEX Industries, Inc., Edison, NJ). The ratio of the signals generated at 340 and 380 nm was used to calculate $[Ca^{2+}]_i$ (nM) by the method of Grynkiewicz et al. (21). Calibration of $[Ca^{2+}]_i$ was performed according to Gelperin et al. (22). The background light intensity in the absence of cells ($F_{340,bk}$; $F_{380,bk}$) was subtracted from the cell signal and used to compute the 340:380 ratio (R) = $(F_{340} - F_{340,bk})$:$(F_{380} - F_{380,bk})$. $R_{min}$ and $R_{max}$ were determined as described by Friel and Tsien (23). DRGs were depolarized with 6 s applications of either elevated $K^+$ Krebs buffer (30–50 mM KCl), or Krebs buffer containing 1 μM capsaicin. The amplitude of the initial peak $[Ca^{2+}]_i$ response to depolarization was measured, and nanomolar $[Ca^{2+}]_i$ calculated from a calibration nomogram. The effect of removing external $Ca^{2+}$ on the KCl-mediated peak $[Ca^{2+}]_i$ response was assessed by perfusion with $Ca^{2+}$-free Krebs buffer containing 1 mM EGTA. The effect of Dyn A on peak $[Ca^{2+}]_i$ was assessed by perfusion of DRGs for 30 s with Krebs buffer containing Dyn A (1 or 3 μM), followed by a 6 seconds perfusion with a depolarizing solution containing both 30 mM KCl and the same concentration of Dyn A. To determine the degree of Dyn A-mediated inhibition, the increase in $[Ca^{2+}]_i$ over basal ($\Delta [Ca^{2+}]_i$) was calculated for both the pre–Dyn A response and the response in the presence of Dyn A by subtracting the basal $[Ca^{2+}]_i$ from peak $[Ca^{2+}]_i$. The percent decrease in the presence of Dyn A was calculated as:

$$100\ (1 - [\Delta \text{ Dyn A } \{\Delta \text{ pre-Dyn A}^{-1}\}])$$

The effect of pertussis toxin was investigated by pretreatment of DRGs with Fura-2 loading medium containing PTX 250 ng $ml^{-1}$ for 3–4 h before recording.

*Statistical analysis.* Peak calcium current densities obtained by analysis of individual recordings were analyzed using the statistical software package GraphPad Prism (GraphPad Software, Inc., San Diego, CA). Significance was determined using two-way ANOVA and the two-tailed Student's *t* test and defined as a $P$ value $< 0.05$ (24).

## Results

*Diabetes was associated with significant enhancement of high-threshold calcium current density ($I_{DCa}$) and decreased nerve conduction velocity.* Diabetic animals demonstrated significant alterations in body weight, blood glucose, glycated hemoglobin, and significant slowing of nerve conduction velocity compared to nondiabetic control animals (Table I). DRG neurons from animals diabetic for 7–10 mo or age-matched nondiabetic controls were prepared as described in Methods, and experiments were performed on neurons 20–40 μm in diameter. After patch rupture, whole-cell, high-threshold calcium currents were elicited at 30 s intervals by depolarizing from a holding potential of −80 mV to +10 mV for 100 ms. Between depolarizations, the neurons were held at −80 mV. Calcium current density ($I_{DCa}$) was calculated by dividing the whole-cell current by the whole-cell capacitance calculated from calibration voltage steps performed immediately after patch rupture. As we have shown previously (9), $I_{DCa}$ increased 20–30% in amplitude during the initial 2–5 min after patch rupture (runup), after which current density decreased at a relatively steady rate (rundown) such that by 20 min after patch rupture, the current amplitude was ~ 60% of the maximum amplitude recorded. Current rundown occurred at a similar rate in diabetic and control neurons (9). High-threshold $I_{DCa}$ in DRG neurons from diabetic animals was significantly enhanced compared to controls (Table II).

*Diabetes was associated with decreased Dyn A–mediated inhibition of high-threshold calcium current density ($I_{DCa}$).* $I_{DCa}$ was elicited at 30-s intervals until the maximum current density was observed (usually between 2 to 5 min after patch rupture). When $I_{DCa}$ had reached maximum levels, a micropipette puffer containing Dyn A was lowered into the bath, and the tip placed within 50 μM of the neuron being recorded. Dyn A was applied for 2 s using air pressure ejection. Currents were elicited immediately before lowering the micropipette (pre–Dyn A), 2 s and 15 s after application of Dyn A (post–Dyn A). In neurons that demonstrated additional inhibition at 15 s compared to 2 s, a second application of Dyn A was performed for 2 s, and currents were elicited 2 s later, then at 30 s intervals until partial or complete recovery of high-threshold $I_{DCa}$ from inhibition was observed (usually within 3–5 min). After drug application, the pipette was immediately removed from the recording bath. Fig. 1 shows the inhibitory effect of Dyn A application on $I_{DCa}$ recorded from diabetic and nondiabetic control DRGs. In Fig. 1 *A*, the effect of 1 μM Dyn A on typical high-threshold calcium currents recorded in a control neuron and a neuron from a diabetic animal is shown. Currents recorded in control DRG neurons were inhibited by Dyn A at concentrations of 1, 3, and 5 μM by 18±3% ($n = 6$), 25±4% ($n = 5$), and 37±7% ($n = 3$), respectively (Fig. 1 *B*). Compared to controls, DRG neurons from diabetic animals demonstrated significantly ($P < 0.05$) less inhibitory effect of Dyn A; 6±2% ($n = 6$), 8±2% ($n = 4$), and 11±3% ($n = 3$) at 1, 3, and 5 μM, respectively. The decreased inhibitory response in diabetic DRGs could not be overcome by increasing the concentration of Dyn A to levels as high as 5 μM. After recovery from Dyn A–mediated inhibition, the irreversible N-type channel blocker ω-conotoxin GVIA (ω-CgTX; 10 μM) was applied for 2 s using a second micropipette lowered into the recording bath. Omega-CgTX decreased control $I_{DCa}$ by 48±4% ($n = 11$) and

*Table I. Nerve Conduction Velocity Decreased in Diabetes*

| | Body weight | Blood glucose | Glycated Hb | NCV |
|---|---|---|---|---|
| | *g* | *mmol/liter* | *%* | *m/s* |
| Control ($n = 7$) | 488.3±6.5 | 5.2±0.1 | 6.0±0.5 | 59.5±0.5 |
| Diabetic ($n = 6$) | 332.4±7.5* | 22.0±0.8‡ | 11.9±1.0* | 45.2±0.5* |

Body weights, plasma glucose levels, glycated hemoglobin (Hb), and nerve conduction velocity (NCV) in 8-mo-old nondiabetic control and diabetic BB/W rats. *$P < 0.05$, ‡$P < 0.01$ by ANOVA.

*Table II. Enhanced Calcium Current Density ($I_{DCa}$) in Diabetes Mellitus*

| | Diameter | Capacitance | Peak $I_{Ca}$ | Peak $I_{DCa}$ |
|---|---|---|---|---|
| | *μm* | *pF* | *nA* | *pA pF$^{-1}$* |
| Control (24) | 27±3 | 24.4±3.3 | 3.97±0.49 | 104.5±26.4 |
| Diabetic (20) | 30±2 | 31.7±2.9 | 6.47±1.02* | 160.2±21.7‡ |

Cell diameter and capacitance calculated as described in Methods. Each value is the mean±SEM of data from (*n*) control and diabetic neurons. *$P < 0.01$, ‡$P < 0.05$ by ANOVA.

diabetic $I_{DCa}$ by 56±7% ($n = 10$). In the presence of ω-CgTX, Dyn A-mediated inhibition was almost abolished in both control and diabetic neurons (Fig. 2). Preincubation with PTX 250 ng ml$^{-1}$ at 37°C for between 3 and 4 h before recording caused a modest, nonsignificant increase in the mean amplitude of peak $I_{DCa}$ elicited in both control (120.6±18.3 pA pF$^{-1}$, $n = 7$) and diabetic DRGs (175.6±28.6 pA pF$^{-1}$, $n = 8$) (compared with Peak $I_{DCa}$ in Table II), and markedly reduced the inhibitory effect of 3 μM Dyn A on $I_{DCa}$ (percent inhibition post-PTX: control 10±2 ($n = 6$); diabetic 5±1 ($n = 4$); not significant).

*Cytosolic calcium $[Ca^{2+}]_i$ studies.* Isolated, dissociated DRGs in a size range similar to those used in electrophysiologic recording were selected and $[Ca^{2+}]_i$ was measured in individual isolated neurons using the Fura-2 method. The neuron diameter was measured using a scale in the microscope ocular. There was no significant difference in DRG diameter between neurons from diabetic animals (36.3±1.8; $n = 27$) and those from age-matched nondiabetic controls (32.6±3.5; $n = 25$). DRGs were perfused with oxygenated Krebs solution for 30 s while basal $[Ca^{2+}]_i$ was monitored, then depolarized by perfusion with 50 mM KCl-containing Krebs buffer for 6 s (Fig. 3 *A*). Application of 50 mM KCl caused an increase in $[Ca^{2+}]_i$ that demonstrated an initial peak, followed by a plateau phase that recovered to basal levels over several minutes. After allowing $[Ca^{2+}]_i$ to recover to basal levels, the neuron was perfused with $Ca^{2+}$-free Krebs buffer containing 1 mM EGTA for 1 min, then re-challenged with 50 mM KCl in $Ca^{2+}$-free Krebs buffer. The $[Ca^{2+}]_i$ response to 50 mM KCl in DRGs from control and diabetic animals was abolished by removal of external $Ca^{2+}$, and restored by re-perfusion with $Ca^{2+}$-containing buffer. The amplitude of the peak response decreased with repeated exposures to elevated KCl. Fig. 3 *B* summarizes the change in peak $[Ca^{2+}]_i$ over basal levels in $Ca^{2+}$-containing, and $Ca^{2+}$-free perfusion media. The Δ peak $[Ca^{2+}]_i$ response (660±46 nM) to 50 mM KCl-mediated depolarization of control DRGs (755±56 nM minus basal $[Ca^{2+}]_i$ of 94 + 25 nM) was abolished in $Ca^{2+}$-free perfusion medium.

*Diabetes was associated with enhanced $[Ca^{2+}]_i$ response to depolarization mediated by elevated KCl and capsaicin.* Neurons from age-matched, nondiabetic controls and diabetic animals were selected and stimulated using the protocol described above. Basal $[Ca^{2+}]_i$ was not significantly different in DRGs from control (94±25 nM) and diabetic (119±12 nM) animals (Fig. 4). When compared to the $[Ca^{2+}]_i$ response elicited by KCl-mediated depolarization of DRGs from control animals (755±56 nM), DRGs from diabetic animals demonstrated a significant increase in the peak $[Ca^{2+}]_i$ response (1033±70; $P < 0.01$) to a 6 s depolarization with 50 mM KCl. Capsaicin perfusion of DRGs from control and diabetic animals elicited an elevation in $[Ca^{2+}]_i$ that was similar in appearance to that stimulated by KCl (Fig. 5 *A*). The mean peak $[Ca^{2+}]_i$ response to perfusion with 1 μM capsaicin was significantly larger ($P <$ 0.05) in DRGs from diabetic animals (835±68 nM) than in DRGs from age-matched controls (647±82 nM) (Fig. 4).

*Diabetes was associated with decreased Dyn A–mediated inhibition of the $[Ca^{2+}]_i$ response to depolarization.* In the experiments testing Dyn A–mediated inhibition, 30 mM KCl, rather than 50 mM was used. Compared to the 50 mM solution, depolarization with 30 mM KCl elicited a $[Ca^{2+}]_i$ response with a peak amplitude ~ 20% smaller than that elicited by 50 mM KCl. The $[Ca^{2+}]_i$ response to 30 mM KCl had little or no plateau phase, shortening the recovery period necessary to achieve basal $[Ca^{2+}]_i$. Using the lower concentration of KCl improved the reproducibility of the $[Ca^{2+}]_i$ response observed with repeated depolarizations during a typical recording session, and minimized the effect of rundown of the $[Ca^{2+}]_i$ response to Dyn A. After a basal recording period, DRGs from either diabetic or control animals were depolarized by perfusion with 30 mM $K^+$-containing Krebs buffer for 6 s (Fig. 5 *A*).

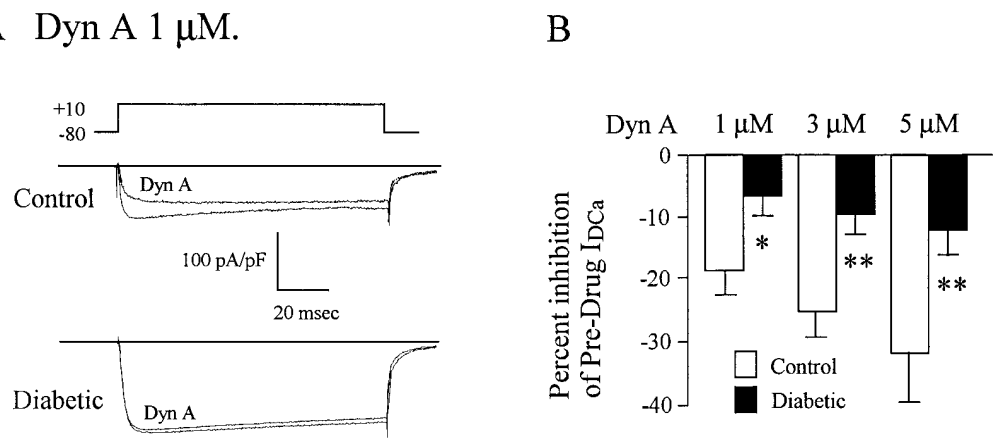


*Figure 1.* Inhibition of high-threshold $I_{DCa}$ by Dyn A was decreased in diabetes. (*A*) Representative calcium currents elicited by depolarization from $V_h = -80$ mV to +10 mV for 100 ms. Currents were elicited before and after application of Dyn A 1 μM for a control and diabetic neuron. (*B*) Dyn A-mediated inhibition of $I_{DCa}$ was significantly less (*$P < 0.05$, **$P < 0.01$) in diabetic DRGs compared to controls. The percent inhibition of $I_{DCa}$ caused by Dyn A application in control and diabetic neurons was calculated as described in Methods for Dyn A applications at 1, 3, and 5 μM. Values are the mean±SEM of (*n*) experiments: Control: 1 μM (6); 3 μM (5); 5 μM (3), Diabetic: 1 μM (6); 3 μM (4); 5 μM (3).

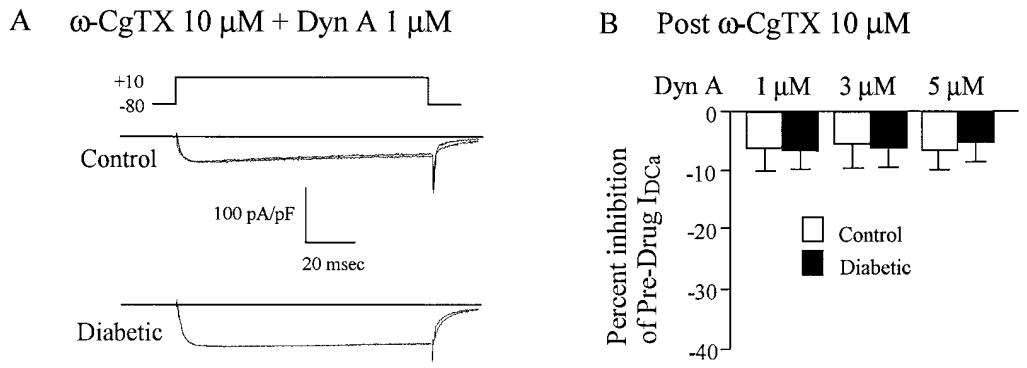


*Figure 2.* Effect of ω-conotoxin GVIA (ω-CgTX; 10 μM) on Dyn A–mediated inhibition of $I_{DCa}$ recorded from diabetic and control DRGs. (*A*) After application of 10 μM ω-CgTX, application of 1 μM Dyn A caused little, or no inhibition in representative currents recorded from control and diabetic DRGs. (*B*) Application of 10 μM ω-CgTX abolished the difference in Dyn A-mediated inhibition of $I_{DCa}$ observed in diabetic DRGs compared to controls. The percent inhibition of $I_{DCa}$ caused by Dyn A application in control and diabetic neurons was calculated as described in Methods for Dyn A applications at 1, 3, and 5 μM. Values are mean±SEM for (*n*) experiments: Control: 1 μM ($n = 4$); 3 μM ($n = 5$); 5 μM ($n = 2$), Diabetic: 1 μM ($n = 4$); 3 μM ($n = 4$); 5 μM ($n = 2$).

The first depolarization was termed the pre–Dyn A response. After recovery from depolarization, DRGs were perfused with Krebs buffer containing Dyn A at concentrations of either 1 or 3 μM for 2 min, then re-challenged with a 6 s perfusion of buffer containing both 30 mM KCl and the same concentration of Dyn A. The magnitude of KCl-mediated elevation in $[Ca^{2+}]_i$ was reduced in the presence of Dyn A and recovered partially or completely after washout of Dyn A. After recovery, neurons remained responsive to other depolarizing agents, as perfusion with buffer containing 1 μM capsaicin elicited a large increase in $[Ca^{2+}]_i$ (Fig. 5 *A*). Only neurons that demonstrated ≥ 50% recovery in $[Ca^{2+}]_i$ amplitude after washout of Dyn A were analyzed, to ensure that the decreased response in the presence of Dyn A was not due simply to rundown of the response with time. Basal $[Ca^{2+}]_i$ was subtracted from the peak KCl-induced depolarization response before, and in the presence of, Dyn A to obtain a Δ peak $[Ca^{2+}]_i$ response. The Δ peak $[Ca^{2+}]_i$ responses to 1 and 3 mM Dyn A, and 3 μM Dyn A after pretreatment with PTX are summarized in Fig. 5 *B*. Dyn A (1 μM) reduced the peak $[Ca^{2+}]_i$ response to elevated KCl-evoked depolarization by 13±4% ($n = 4$) in neurons from diabetic animals, which was significantly less than the reduction (27±5%; $n = 6$) observed in age-matched control neurons ($P < 0.05$). Dyn A (3 μM)-mediated inhibition of the Δ peak $[Ca^{2+}]_i$ response in DRGs from diabetic animals was also significantly less (33±8%; 710±62 nM; $P < 0.01$) than that observed in age-matched controls (73±6%; 247±78 nM) (Fig. 4 *B*). Preincubation with PTX 250 ng $ml^{-1}$ for 3–4 h before recording abolished the inhibitory $[Ca^{2+}]_i$ response to Dyn A in both diabetic (7±5%) and control (8±6%) DRGs.

## Discussion

Our results suggest that diabetes mellitus is associated with decreased Dyn A–mediated inhibition of calcium influx via neuronal calcium channels. We believe that this is the first direct demonstration that opioid-mediated regulation of calcium channels is attenuated in neurons from diabetic animals. Both increased and decreased antinociceptive responses to opiate agonists have been described in diabetes mellitus (13). The effect of diabetes on opiate-mediated inhibition of tail-flick and other avoidance responses may be related to the degree of hyperglycemia (25, 26). Differential effects of opiates have been reported in the central and peripheral nervous system, with su-

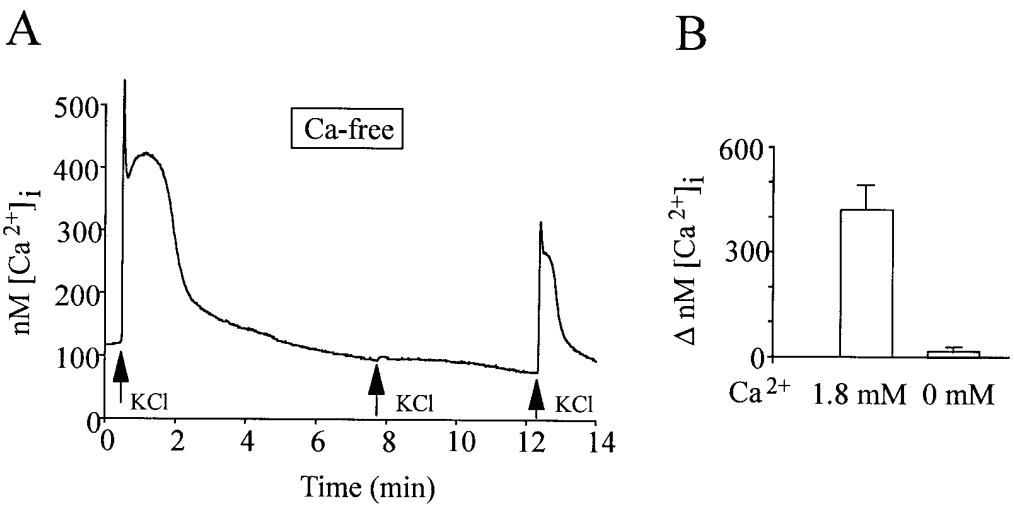


*Figure 3.* $[Ca^{2+}]_i$ response to KCl depolarization was dependent on entry of external $Ca^{2+}$. (*A*) Representative Fura-2 recording obtained from a 10-mo-old control animal showing the $[Ca^{2+}]_i$ response to 50 mM KCl depolarization for 6 s in Krebs perfusion medium containing 1.8 mM $Ca^{2+}$ or $Ca^{2+}$-free Krebs medium (0 mM $Ca^{2+}$ supplemented with 1.0 mM EGTA). In $Ca^{2+}$-containing medium, 50 mM KCl induced a peak in $[Ca^{2+}]_i$ followed by a plateau phase that decreased to basal levels with time. The response to KCl was abolished when $Ca^{2+}$-free buffer was perfused during the interval indicated by the box and was restored with re-perfusion of $Ca^{2+}$-containing buffer. (*B*) The mean±SEM peak $[Ca^{2+}]_i$ response to KCl-mediated depolarization in calcium-containing and calcium-free medium for eight neurons.

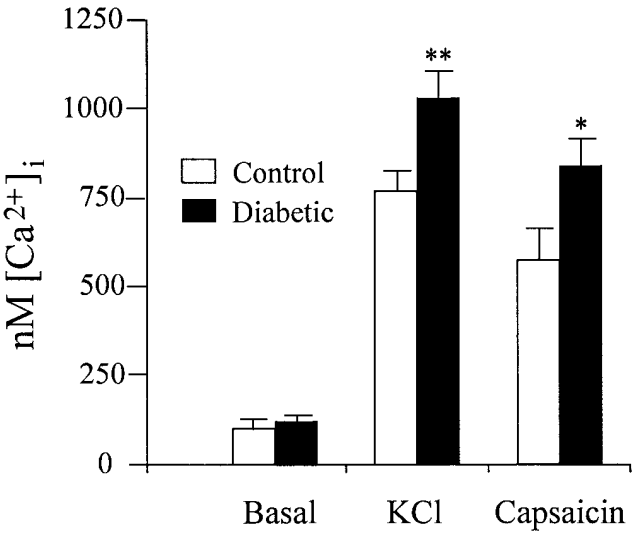


*Figure 4.* The $[Ca^{2+}]_i$ response to KCl- and capsaicin-mediated depolarization was enhanced in diabetes. Basal $[Ca^{2+}]_i$ measured before the first KCl-mediated depolarization was not significantly different in DRGs from diabetic and control animals. Application of 50 mM KCl- or 1 μM capsaicin-containing Krebs buffer for 6 s caused an increase in peak $[Ca^{2+}]_i$ that was significantly ($^*P < 0.05$, $^{**}P < 0.01$) higher in DRG neurons from diabetic animals ($n = 9$) than neurons from age-matched controls ($n = 9$). Values are mean±SEM.

persensitivity to opiate stimulation of δ-1 receptors documented in the central nervous system (27), while μ and κ opiate responses at the spinal level appear to be decreased in diabetes (13), a finding which is consistent with our observation that Dyn A–mediated inhibition of calcium influx is decreased in spinal sensory ganglia.

Endogenous opiates, such as Dyn A, appear to play a physiologic role in modulation of calcium influx in DRGs, as Dyn A is present in neurons within the DRG and dorsal horn of the spinal cord (12). In addition, μ and κ receptors are present on DRGs, as evidenced by mRNA production (28) and functional response to stimulation by selective μ and κ agonists and antagonists (17). Decreased opiate receptor expression could explain the loss of opiate responsiveness in diabetes, and impaired vagal transport of opiate receptors has been demonstrated in streptozotocin-induced diabetic rats (14). However, elevated beta endorphin binding sites on muscle have been documented in the type II obese diabetic mouse model (29), and neuronal opiate receptor binding in the brain is not altered in spontaneously diabetic or streptozotocin-induced diabetic rats (30). Alternatively, altered opiate receptor coupling to ion channels might be present in diabetes. To examine the possibility that opiate modulation of calcium channels was altered in diabetes, we used the opiate receptor agonist Dyn A. Dyn A inhibits high-threshold, voltage-activated calcium channels on DRGs via coupling to PTX-sensitive inhibitory ($G_o$-type) G proteins (16). Dyn A–mediated inhibition of voltage-activated calcium currents was significantly reduced in diabetes, suggesting that either opiate receptor number was reduced or that the signal transduction pathway coupling the receptor to the channel was altered. The inhibitory effect of Dyn A on DRG calcium currents involves both κ and μ receptors (16), with activation of κ receptors predominating at doses at or less than 1 μM, whereas doses above 1 μM stimulate predominantly μ receptors (17). In our studies, application of ω-CgTX abolished the differential inhibitory effect of Dyn A on currents recorded from diabetic DRGs compared to controls, however application of Dyn A still produced a small amount of inhibition (6–8%) in both control and diabetic DRGs. A small proportion (< 20%) of Dyn A–mediated inhibition of high-threshold calcium currents in DRG neurons has been shown to involve P and Q type calcium channels, in addition to N-type (31), therefore it is likely that the residual inhibition observed in our studies after application of ω-CgTX was due to an effect of Dyn A on P and Q channel currents. Our results imply that the inhibitory effect of Dyn A on these channels is not affected by diabetes. We studied neurons from DRGs in the size range 20–40 μm, since our previous studies demonstrated that neu-

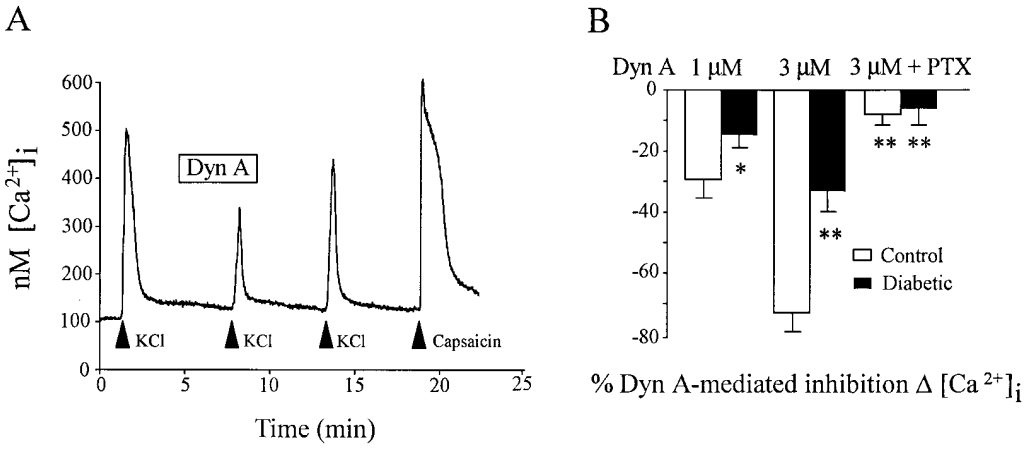


*Figure 5.* Dyn A-mediated inhibition of KCl-stimulated increase in peak $[Ca^{2+}]_i$ was decreased in diabetes. (*A*) Representative Fura-2 experiment recorded in a DRG from a diabetic animal showing the peak $[Ca^{2+}]_i$ response to 30 mM KCl depolarization elicited before, during, and after perfusion with 1 μM Dyn A–containing Krebs buffer as outlined in Methods. Application of Dyn A during the interval indicated by the box decreased the peak amplitude of the $[Ca^{2+}]_i$ response to 30 mM KCl. After washout of Dyn A–containing buffer, a third application of KCl demonstrated partial recovery of the $[Ca^{2+}]_i$ response. Application of 1 μM capsaicin at the end of the experiment elicited a $[Ca^{2+}]_i$ response. (*B*) Percent inhibition of the peak $[Ca^{2+}]_i$ response to KCl in the presence of 1 and 3 μM Dyn A was calculated as described in Methods. DRGs from diabetic animals demonstrated a significantly decreased $[Ca^{2+}]_i$ response compared to controls ($^*P < 0.05$, $^{**}P < 0.01$). Preincubation with PTX for 3 h before recording abolished the inhibitory $[Ca^{2+}]_i$ response to 3 μM Dyn A in both control and diabetic neurons. Values are mean±SEM of (*n*) experiments: Control: 1 μM Dyn A (3); 3 μM Dyn A (5); 3 μM Dyn + PTX (4), Diabetic: 1 μM Dyn A (4); 3 μM Dyn A (4); 3 μM Dyn + PTX (4).

rons in this size range were predominantly (80%) capsaicin sensitive (9). In addition to nociception, the capsaicin-sensitive population of small to medium sized DRG neurons likely subserve other sensory modalities such as stretch and chemosensation (32, 33), therefore the enhancement in $I_{DCa}$ and $[Ca^{2+}]_i$ observed in this neuronal population implies alterations in these other sensory modalities in diabetes.

Activation of voltage-gated calcium channels in the cell outer membrane leads to a cascade of well-described intracellular events including: synaptic neurotransmitter release, secretion, release of calcium from intracellular pools, and activation of other ion channels. Recently, attention has focused on mechanisms by which calcium homeostasis is altered, as the resultant elevations in cytosolic calcium ($[Ca^{2+}]_i$) may contribute to neuronal cell injury and death (8, 10). Our previous studies suggested that diabetes mellitus might alter intracellular pathways regulating calcium channels and lead to elevation in cytosolic calcium levels in response to depolarization. Therefore, one of the objectives of the present study was to examine whether the increased calcium currents observed in diabetes correlated with an increase in $[Ca^{2+}]_i$. Our results indicate that the increase in calcium currents in diabetes is associated with an enhanced cytosolic calcium response to depolarization mediated by elevated KCl and capsaicin. Diabetes was not associated with a significant elevation in basal $[Ca^{2+}]_i$. Depolarization with elevated KCl and capsaicin caused a significantly greater change in the peak $[Ca^{2+}]_i$ in DRGs from diabetic animals compared to age-matched controls. Although measurements of $[Ca^{2+}]_i$ and calcium currents were not performed on the same cell, there was a strong similarity in the magnitude of the increase in calcium currents and $[Ca^{2+}]_i$, thus the increase in $[Ca^{2+}]_i$ observed in diabetes was likely associated with the enhanced calcium currents observed during depolarization (11). In addition, neurons from diabetic animals also demonstrated an increase in $[Ca^{2+}]_i$ response to capsaicin, which acts via a ligand-gated pathway to cause calcium entry in neurons (34), indicating that both non–receptor-induced (KCl-mediated depolarization) and ligand-gated calcium entry are affected by diabetes in a parallel manner. The physiological concentration at which Dyn A acts on opiate receptors in spinal ganglia is unknown. At the same concentrations used in the electrophysiologic studies in this publication, and in previous studies (15, 35), Dyn A caused a substantial reduction ($> 70\%$ with 3 $\mu$M Dyn A) in KCl-mediated increased $[Ca^{2+}]_i$ in control neurons, which was significantly less in neurons from diabetic animals. At this dose, Dyn A acted via an opiate pathway, as the effects were blocked by naloxone (15).

Because inhibitory G proteins modulate opiate-mediated inhibition of calcium influx, alterations in guanine nucleotide-binding (G) protein coupling to calcium channels may underlie the enhanced influx and cytosolic calcium present in diabetes. Decreased G protein levels and reduced functional activity of inhibitory G proteins have been described in non-neuronal tissues of a diabetic rat model (36). In the present study, the effects of Dyn A on calcium current density and $[Ca^{2+}]_i$ response to depolarization in diabetic neurons were abolished by pertussis toxin, indicating that calcium channels remained coupled to inhibitory G proteins in diabetes. Finally, diabetes could affect other components of signal transduction pathways, such as protein kinase–mediated phosphorylation of various components of the receptor-effector system. Of interest, intracellular administration of cAMP-dependent protein kinase and protein kinase C (PKC) increase high-threshold calcium currents in DRG neurons (15, 37, 38), and diabetes is associated with elevated levels of PKC isoforms (39). The role of phosphorylation remains to be elucidated, however, as decreased PKC levels have been correlated with impaired nerve conduction in diabetes (40).

Alterations in intracellular calcium homeostasis resulting in increased $[Ca^{2+}]_i$ have been documented in several models of diabetes (8). Abnormalities described include increased vascular responsiveness to agents such as Bay K 8644 that increase calcium influx (41) and decreased intracellular re-sequestration secondary to decreased $Ca^{2+}$-$Mg^{2+}$ATPase activity (42). Increased total calcium content has been described in sciatic nerves from streptozotocin-induced diabetic rats (43). The pathophysiologic significance and mechanism(s) underlying impaired calcium signaling are unclear. Increased cytosolic calcium has been demonstrated in various models of neuronal injury, and agents that decrease calcium influx have ameliorated loss of neuronal function in models of neuronal injury (10). Preliminary reports of improvement in diabetic nerve conduction velocity with administration of the L-type calcium channel blocker nimodipine (44) suggest that the effect of increased calcium influx in diabetes may be injurious. However, modest elevation of $[Ca^{2+}]_i$ appears to be beneficial to neuronal growth, as exposure to moderately elevated KCl prevents neuronal loss due to programmed cell death or apoptosis (45). We favor the interpretation that the observed enhancement in calcium influx in diabetes is pathophysiologic rather than compensatory because, in our previous studies (9), the magnitude of enhancement in calcium influx increased with the duration of diabetes and paralleled the deterioration in nerve conduction velocity. Long-term administration of an aldose reductase inhibitor to diabetic animals was associated with normalization of nerve conduction velocity and neuronal calcium influx. In light of these findings, it would be interesting to determine whether aldose reductase treatment reversed the decreased effectiveness of opiate-mediated inhibition of calcium signaling in diabetes.

In summary, these results provide evidence of a cellular mechanism that may contribute to the decreased opiate sensitivity reported in sensory pathways in diabetes mellitus. Opiate-mediated inhibition of both voltage-activated calcium currents ($I_{DCa}$) and $[Ca^{2+}]_i$ response to depolarization was significantly decreased in sensory neurons from diabetic animals, compared to neurons from nondiabetic, age-matched controls. The congruent changes in calcium current density and elevated KCl/capsaicin-mediated increases in $[Ca^{2+}]_i$ suggest that an intracellular signal transduction mechanism common to both responses is impaired in diabetes. This abnormality may contribute to the mechanism(s) that underlie the pathophysiologic changes associated with diabetic neuropathy.

## Acknowledgments

The authors gratefully acknowledge the expert technical assistance of Brian Dzwonek, David Mann, Andrew Merry, and Helen Ristic.

These studies were supported by a Medical Council of Canada Centennial Fellowship, Michigan Peptide Research Center Pilot Feasibility Award (K.E. Hall), Veterans Administration Merit Award, National Institutes of Health grant #R29DK45820-01, University of Michigan Diabetes Research and Training Center Pilot Feasibility

Award (J.W. Wiley), and National Institutes of Health grant #DK43884 (A.A.F. Sima).

## References


1. Bischoff, A. 1973. Ultrastructural pathology of peripheral nervous system in early diabetes. *In* Vascular and Neurologic Changes in Early Diabetes. R.A. Camerini-Davalos, and H.S. Cole, editors. Academic Press, New York. 441–449.

2. Behse, F., F. Buchtal, and F. Carlsen. 1977. Nerve biopsy and conduction studies in diabetic neuropathy. *J. Neurol. Neurosurg. Psych.* 40:1072–1082.

3. Brismar, T., and A.A.F. Sima. 1981. Changes in the nodal function in nerve fibers of the spontaneously diabetic BB-Wistar rat: potential clamp analysis. *Acta Physiol. Scand.* 113:499–506.

4. Yasuda, H., and P.J. Dyck. 1987. Abnormalities of endoneurial microvessels and sural nerve pathology in diabetic neuropathy. *Neurology.* 37:20–28.

5. Sima, A.A.F., A. Prashar, W.-X. Zhang, S. Chakrabarti, and D.A. Greene. 1990. Preventative effect of long term aldose reductase inhibition (Ponalrestat) on nerve conduction and sural nerve structure in the spontaneously diabetic BB-rat. *J. Clin. Invest.* 85:1410–1420.

6. Sima, A.A.F., and T. Brismar. 1985. Reversible diabetic nerve dysfunction: structural correlates to electrophysiologic abnormalities. *Ann. Neurol.* 18: 21–29.

7. Greene, D.A., S.A. Lattimer, and A.A.F. Sima. 1987. Sorbital, phosphoinositides, and sodium-potassium-ATPase in the pathogenesis of diabetic complications. *N. Engl. J. Med.* 316:599–606.

8. Levy, J., J.R. Gavin, III, and J.R. Sowers. 1994. Diabetes mellitus: a disease of abnormal cellular calcium metabolism. *Am. J. Med.* 96:260–273.

9. Hall, K.E., A.A.F. Sima, and J. Wiley. 1995. Voltage-dependent calcium currents are enhanced in rat dorsal root ganglion neurons from the Bio/Bred Worcester diabetic rat. *J. Physiol. (Lond.).* 486:313–322.

10. Nicotera, P., G. Bellomo, and S. Orrenius. 1992. Calcium-mediated mechanisms in chemically induced cell death. *Annu. Rev. Pharmacol. Toxicol.* 32:449–470.

11. Thayer, S., and R. Miller. 1990. Regulation of the intracellular free calcium concentration in single rat dorsal root ganglion neurons in vitro. *J. Physiol. (Lond.).* 425:85–115.

12. Pohl, M., J.J. Benoliel, S. Bourgoin, M.C. Lombard, A. Mauborgne, H. Taquet, A. Carayon, J.M. Besson, F. Cesselin, and M. Hamon. 1990. Regional distribution of calcitonin gene-related peptide-, substance P-, cholecystokinin-, Met5-enkephalin-, and dynorphin A (1-8)-like materials in the spinal cord and dorsal root ganglia of adult rats: effects of dorsal rhizotomy and neonatal capsaicin. *J. Neurochem.* 55:1122–1130.

13. Kamei, J., N. Kawashima, H. Hitosugi, M. Misawa, H. Nagase, and Y. Kasuya. 1993. Effect of diabetes on the antinociceptive effect of beta-endorphin. *Brain Res.* 619:76–80.

14. Laduron, P.M., and P.F. Janssen. 1986. Impaired axonal transport of opiate and muscarinic receptors in streptozocin-diabetic rats. *Brain Res.* 380: 359–362.

15. Gross, R.A., H.C. Moises, M.D. Uhler, and R.L. Macdonald. 1990. Dynorphin A and cAMP-dependent protein kinase independently regulate neuronal calcium currents. *Proc. Natl. Acad. Sci. USA.* 87:7025–7029.

16. Moises, H.C., K.I. Rusin, and R.L. Macdonald. 1994. Mu-opioid receptor-mediated reduction of neuronal calcium current occurs via a $G_o$-type GTP binding protein. *J. Neurosci.* 14:3842–3851.

17. Moises, H.C., K.I. Rusin, and R.L. Macdonald. 1994. Mu- and kappa-opioid receptors selectively reduce the same transient components of high-threshold calcium current in rat dorsal root ganglion sensory neurons. *J. Neurosci.* 14:5903–5916.

18. Hall, K.E., D. Mann, and J. Wiley. 1994. Diabetes is associated with altered cytosolic calcium regulation in primary afferent neurons. *Gastroenterology.* 106:813*a.* (Abstr.)

19. Sima, A.A.F. 1983. The development and structural characterization of the neuropathies in the BB-Wistar rat. *Metab. Clin. Invest.* 32(Suppl. 1):106–111.

20. Hamill, O.P., A. Marty, E. Neher, B. Sakmann, and F.J. Sigworth. 1981. Improved patch-clamp techniques for high-resolution current recording from cells and cell-free membrane patches. *Pflugers Arch.* 391:85–100.

21. Grynkiewics, G., M. Poenie, and R.Y. Tsien. 1985. A new generation of $Ca^{2+}$ indicators with greatly improved fluorescence properties. *J. Biol. Chem.* 260:3440–3450.

22. Gelperin, D., D. Mann, J. del Valle, and J.W. Wiley. 1994. Bradykinin (Bk) increases cytosolic calcium in cultured rat myenteric neurons via Bk-2 type receptors coupled to mobilization of extracellular and intracellular sources of calcium: evidence that calcium influx is prostaglandin dependent. *J. Pharmacol. Exp. Ther.* 271:507–514.

23. Friel, D.D., and R.W. Tsien. 1992. A caffeine and ryanodine-sensitive $Ca^{2+}$ store in bullfrog sympathetic neurons modulates the effects of $Ca^{2+}$ entry on $[Ca^{2+}]_i$. *J. Physiol. (Lond.).* 450:217–246.

24. Mendenhall, W. 1975. Introduction to Probability and Statistics, 4th ed., Duxbury Press, North Scltuate, MA. 460 pp.

25. Lee, J.H., and R. McCarty. 1990. Glycemic control of pain threshold in diabetic and control rats. *Physiol. Behav.* 47:225–230.

26. Brase, D.A., Y.H. Han, and W.L. Dewey. 1987. Effects of glucose and diabetes on binding of naloxone and dihydromorphine to opiate receptors in mouse brain. *Diabetes.* 36:1173–1177.

27. Kamei, J., N. Kawashima, and Y. Kasuya. 1992. Paradoxical analgesia produced by naloxone in diabetic mice is attributable to supersensitivity of delta-opioid receptors. *Brain Res.* 592:101–105.

28. Maekawa, K., M. Minami, K. Yabuuchi, T. Toya, Y. Katao, Y. Hosoi, T. Onogi, and M. Satoh. 1994. In situ hybridization study of mu- and kappa-opioid receptor mRNAs in the rat spinal cord and dorsal root ganglia. *Neurosci. Lett.* 168:97–100.

29. Hughes, S., and M.E. Smith. 1993. Beta-endorphin and ACTH receptors in skeletal muscles in diabetes mellitus. *Ann. NY Acad. Sci.* 680:542–544.

30. Brase, D.A., Y.H. Han, and W.L. Dewey. 1987. Effects of glucose and diabetes on binding of naloxone and dihydromorphine to opiate receptors in mouse brain. *Diabetes.* 36:1173–1177.

31. Konstantin, I.R., and H.C. Moises. 1995. Mu-opioid receptor activation reduces multiple components of high-threshold calcium current in rat sensory neurons. *J. Neurosci.* 15:4315–4327.

32. Lorez, H.P., G. Haeusler, and L. Aeppli. 1983. Substance P neurones in medullary baroreflex areas and baroreflex function of capsaicin-treated rats. Comparison with other primary afferent systems. *Neuroscience.* 8:507–523.

33. Stein, R.D., S. Genovesi, K.T. Demarest, and L.C. Weaver. 1986. Capsaicin treatment attenuates the reflex excitation of sympathetic activity caused by chemical stimulation of intestinal afferent nerves. *Brain Res.* 397:145–151.

34. Bleakman, D., J.R. Brorson, and R.J. Miller. 1990. The effect of capsaicin on voltage-gated calcium currents and calcium signals in cultured dorsal root ganglion cells. *Br. J. Pharmacol.* 101:423–431.

35. Gross, R.A., and R.L. Macdonald. 1987. Dynorphin A selectively reduces a large transient (N-type) calcium current of mouse dorsal root ganglion neurons in cell culture. *Proc. Natl. Acad. Sci. USA.* 84:5469–5473.

36. Bushfield, M., S.L. Griffiths, G.J. Murphy, N. Pyne, J.T. Knowler, G. Milligan, P.J. Parker, S. Mollner, and M.D. Houslay. 1990. Diabetes-induced alterations in the expression, functioning and phosphorylation state of the inhibitory guanine nucleotide regulatory protein $G_{i2}$ in hepatocytes. *Biochem. J.* 271: 365–372.

37. Yang, J., and R.W. Tsien. 1993. Enhancement of N- and L-type calcium channel currents by protein kinase C in frog sympathetic neurons. *Neuron.* 10: 127–136.

38. Hall, K.E., M. Browning, E.M. Dudek, and R.L. Macdonald. 1995. Enhancement of high threshold calcium currents in rat primary afferent neurons by constitutively active protein kinase C. *J. Neurosci.* 15:6069–6076.

39. Inoguchi, T., R. Battan, E. Handler, J.R. Spotsman, W. Heath, and G.L. King. 1992. Preferential elevation of protein kinase C isoform βII and diacylglycerol levels in the aorta and heart of diabetic rats: differential reversibility to glycemic control by islet cell transplantation. *Proc. Natl. Acad. Sci. USA.* 89: 11059–11063.

40. Kim, J., E.H. Rushovich, T.P. Thomas, T. Uedat, B.W. Agranoff, and D.A. Greene. 1991. Diminished specific activity of cytosolic protein kinase C in sciatic nerve of streptozotocin-induced diabetic rats and its correction by dietary *myo*-inositol. *Diabetes.* 40:1545–1554.

41. White, R.E., and G.O. Carrier. 1990. Vascular contraction induced by activation of membrane calcium ion channels is enhanced in streptozotocin-diabetes. *J. Pharm. Exp. Ther.* 253:1057–1062.

42. Heliger, C.E., A. Prakash, and J.H. McNeill. 1987. Alterations in cardiac sarcolemmal $Ca^{2+}$ pump activity during diabetes mellitus. *Am. J. Physiol.* 252: H540–H544.

43. Greene, D.A., and S.A. Lattimer. 1983. Impaired rat sciatic nerve sodium-potassium adenosine triphosphatase in acute streptozotocin diabetes and its correction by dietary myoinositol supplementation. *J. Clin. Invest.* 72:1058–1063.

44. Kappelle, A.C., B. Bravenboer, J. Traber, D.W. Erkelens, and W.H. Gispen. 1992. The $Ca^{2+}$ antagonist nimodipine counteracts the onset of an experimental neuropathy in streptozotocin-induced diabetic rats. *Br. J. Pharmacol.* 111:887–893.

45. Franklin, J.L., and E.M. Johnson, Jr. 1994. Elevated intracellular calcium blocks programmed neuronal death. *Ann. NY Acad. Sci.* 747:195–204.